

Letter to the Editor

## Vibration analysis of buckled thin-walled beams with open sections

F. Mohri<sup>a,c,\*</sup>, L. Azrar<sup>b</sup>, M. Potier-Ferry<sup>c</sup>

<sup>a</sup>*IUT Nancy-Brabois, Département Génie Civil, Université Nancy 1, 54601 Villers les Nancy, France*

<sup>b</sup>*Equipe MMPM, Faculté des Sciences et Techniques de Tanger, Université Abdelmalek Essaadi, BP 416, Tanger, Morocco*

<sup>c</sup>*LPMM, UMR CNRS 7554, ISGMP, Université de Metz, Ile du Saulcy, 57045 Metz, France*

Received 20 January 2003; accepted 9 October 2003

### 1. Introduction

Thin-walled beams with open sections constitute basic parts of many complex steel structures and are extensively used in engineering applications when requirements of weight saving are of primary importance. Due to their particular shapes, these structures are highly sensitive to torsion and to imperfections. The instabilities are then the most important phenomena that must be accounted for in the design. Nevertheless, it is well known that buckling does not always mean failure. Therefore, it is necessary to understand the post-buckling behaviour and vibration characteristics of buckled thin-walled structures under various loads. Although the vibration behaviour of these structures has significant applications in structural engineering, the work done in this area is generally limited to the pre-buckling range [1,2] and research on the vibration of post-buckled thin-walled elements has received scant attention.

A non-linear model which accounts for non-linear warping, bending–bending and torsion–bending couplings has been developed for the non-linear analysis of thin-walled elements with presence of instabilities. Based on this model, the post-buckling behaviour of thin-walled beams under both axial and lateral loads has been investigated [3,4]. This model is extended here to non-linear dynamic analysis. The Galerkin's method is used and a non-linear algebraic system is obtained for the static equilibrium at moderate displacements. The post-buckled solutions are performed using the Newton–Raphson iterative method. Using the tangent stiffness matrix derived from the static solution, the small vibration analysis is carried out in both the pre- and post-buckling regions. For fundamental frequency analyses, the load–frequency interactions are demonstrated for various shapes at large ranges of loads. Closed-form relationships for the

---

\*Corresponding author. IUT Nancy-Brabois, Département Génie Civil, Université Nancy 1, 54601 Villers les Nancy, France. Tel.: +33-383-682577; fax: +33-383-682532.

*E-mail address:* [foudil.mohri@iutnb.uhp-nancy.fr](mailto:foudil.mohri@iutnb.uhp-nancy.fr) (F. Mohri).

eigenfrequencies of bisymmetric and mono-symmetric sections are presented and an eigenvalue problem is formulated for general section shapes.

## 2. Mathematical formulation

### 2.1. Kinematics of the model

In Fig. 1, is shown a straight and undeformed thin-walled beam with an open section that will be considered in this study. The orthogonal cartesian co-ordinate ( $G, x, y, z$ ) is considered where the  $x$ -axis is parallel to the length of the beam and  $G$  is the centre of the cross-section. The shear centre with co-ordinates  $(y_c, z_c)$  in  $Gyz$  is denoted  $C$ . Consider  $M$ , a point on the section contour with its co-ordinates  $(y, z, \omega)$ , where  $\omega$  is the sectorial co-ordinate of the point used in Vlasov’s model for non-uniform torsion. Based on the usual assumptions of the theory of thin-walled elements, the displacement components of  $M$  can be derived from those of the shear centre, as extensively demonstrated in Ref. [3]:

$$u_M = u - y(v' \cos \theta_x + w' \sin \theta_x) - z(w' \cos \theta_x - v' \sin \theta_x) - \omega \theta'_x, \tag{1}$$

$$v_M = v - (z - z_c) \sin \theta_x - (y - y_c)(1 - \cos \theta_x), \tag{2}$$

$$w_M = w + (y - y_c) \sin \theta_x - (z - z_c)(1 - \cos \theta_x), \tag{3}$$

where differentiation with respect to the axial co-ordinate  $x$  is denoted by  $(\prime)$ . Now recall that Vlasov’s relations can be obtained from (1) to (3) using the approximation  $(\cos \theta_x = 1)$  and  $(\sin \theta_x = \theta_x)$  and disregarding the resulting non-linear terms. In beam theory, it is admitted that the axial displacement  $u_M$  is much smaller than  $v_M$  and  $w_M$ . Based on this assumption, the Green strain-tensor components are simplified to

$$\epsilon_{xx} = u'_M + \frac{1}{2}((u'_M)^2 + (v'_M)^2 + (w'_M)^2) \approx u'_M + \frac{1}{2}((v'_M)^2 + (w'_M)^2), \tag{4}$$

$$\epsilon_{xy} = \frac{1}{2} \left( \frac{\partial u_M}{\partial y} + \frac{\partial v_M}{\partial x} + \frac{\partial v_M}{\partial x} \frac{\partial v_M}{\partial y} + \frac{\partial w_M}{\partial x} \frac{\partial w_M}{\partial y} \right), \tag{5}$$

$$\epsilon_{xz} = \frac{1}{2} \left( \frac{\partial u_M}{\partial z} + \frac{\partial w_M}{\partial x} + \frac{\partial v_M}{\partial x} \frac{\partial v_M}{\partial z} + \frac{\partial w_M}{\partial x} \frac{\partial w_M}{\partial z} \right). \tag{6}$$

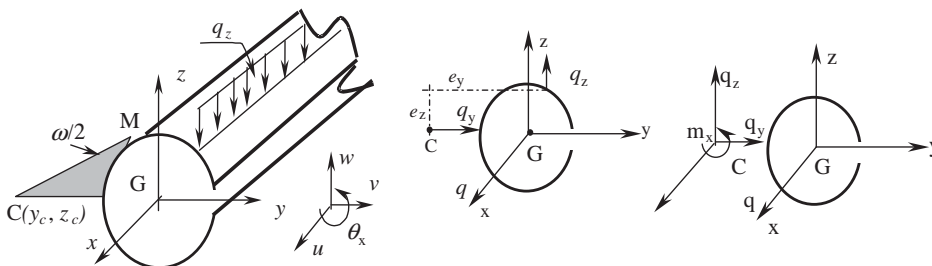


Fig. 1. An open section beam with displacement and load components.

The insertion of relationships (1)–(3) into (4)–(6) leads to the following expressions:

$$\varepsilon_{xx} = \varepsilon_1 + \varepsilon_2 \quad (7a)$$

in which

$$\varepsilon_1 = u' - y(v'' \cos \theta_x + w'' \sin \theta_x) - z(w'' \cos \theta_x - v'' \sin \theta_x) - \omega \theta_x'', \quad (7b)$$

$$\varepsilon_2 = \frac{1}{2}(v'^2 + w'^2 + R^2 \theta_x'^2) - y_C \theta_x'(w' \cos \theta_x - v' \sin \theta_x) + z_C \theta_x'(v' \cos \theta_x + w' \sin \theta_x), \quad (7c)$$

$$\varepsilon_{xy} = -\frac{1}{2}\left(z - z_C + \frac{\partial \omega}{\partial y}\right) \theta_x'; \quad \varepsilon_{xz} = \frac{1}{2}\left(y - y_C - \frac{\partial \omega}{\partial z}\right) \theta_x', \quad (8, 9)$$

where

$$R^2 = (y - y_C)^2 + (z - z_C)^2.$$

## 2.2. Variational formulation and equations of motion

The governing static and dynamic equations of geometrically non-linear theory of thin-walled structures can be obtained from the variational formulation of the strain energy, the external load work and the kinetic energy. The variation of the strain energy of the system has been derived and is given by

$$\begin{aligned} \delta U = & \int_L N(\delta u' + \delta v'(v' + y_C \theta_x' \sin \theta_x + z_C \theta_x' \cos \theta_x) + \delta w'(w' - y_C \theta_x' \cos \theta_x + z_C \theta_x' \sin \theta_x)) \, dx \\ & + \int_L N \delta \theta_x (y_C (w' \theta_x' \sin \theta_x + v' \theta_x' \cos \theta_x) + z_C (w' \theta_x' \cos \theta_x - v' \theta_x' \sin \theta_x)) \, dx \\ & + \int_L N \delta \theta_x' (y_C (-w' \cos \theta_x + v' \sin \theta_x) + z_C (v' \cos \theta_x + w' \sin \theta_x)) \, dx \\ & - \int_L M_y (\delta w'' \cos \theta_x - \delta v'' \sin \theta_x) \, dx + \int_L M_y (w'' \sin \theta_x + v'' \cos \theta_x) \delta \theta_x \, dx \\ & + \int_L M_z (\delta v'' \cos \theta_x + \delta w'' \sin \theta_x) \, dx + \int_L M_z (w'' \cos \theta_x - v'' \sin \theta_x) \delta \theta_x \, dx \\ & + \int_L B_\omega \delta \theta_x'' \, dx + \int_L M_R \theta_x' \delta \theta_x' \, dx + \int_L M_{sv} \delta \theta_x' \, dx, \end{aligned} \quad (10)$$

where  $N$  is the axial force,  $M_y$  and  $M_z$  are the bending moments,  $B_\omega$  is the bimoment and  $M_{sv}$  is the St-Venant torsion moment and  $M_R$  is a higher order stress resultant. They are defined in Ref. [3]. Various types of external loads may be applied to the element. The external load can be expressed by the components  $q_x$ ,  $q_y$  and  $q_z$  and a torsion moment  $m_x$ . The virtual work due to the external loads is given by

$$\delta W = \int_L (q_x \delta u + q_y \delta v + q_z \delta w + m_x \delta \theta_x) \, dx. \quad (11a)$$

Here, the torsion moment  $m_x$  is related to load eccentricities  $q_z$  from the shear centre as indicated in Fig. 1 and is formulated as demonstrated in Ref. [4] by

$$m_x = q_z(e_y \cos \theta_x - e_z \sin \theta_x) \tag{11b}$$

in which  $e_y$  and  $e_z$  are the eccentricities of the applied load  $q_z$  with respect to the shear centre. The  $q_z$  load may induce torsion moment in first or second order considerations, depending on the eccentricities  $e_y$  and  $e_z$ . According to (11b), the virtual work (11a) becomes:

$$\delta W = \int_L (q_x \delta u + q_y \delta v + q_z \delta w + q_z(e_y \cos \theta_x - e_z \sin \theta_x) \delta \theta_x) dx. \tag{11c}$$

The kinetic energy of a straight thin-walled beam with constant density is given by

$$\begin{aligned} T &= \frac{1}{2} \int_L \int_A \rho \left( \left( \frac{\partial u_M}{\partial t} \right)^2 + \left( \frac{\partial v_M}{\partial t} \right)^2 + \left( \frac{\partial w_M}{\partial t} \right)^2 \right) dA dx \\ &= \frac{1}{2} \int_L m \left( \left( \frac{\partial u_M}{\partial t} \right)^2 + \left( \frac{\partial v_M}{\partial t} \right)^2 + \left( \frac{\partial w_M}{\partial t} \right)^2 \right) dx, \end{aligned} \tag{12}$$

where  $\rho$  is the material density and  $m$  denotes the mass density of the element. Based on relationships (1)–(3), and after neglecting the rotary inertia terms, the kinetic energy is

$$T = \frac{1}{2} \int_L m \left( \left( \frac{\partial u}{\partial t} \right)^2 + \left( \frac{\partial v}{\partial t} \right)^2 + \left( \frac{\partial w}{\partial t} \right)^2 + I_0 \left( \frac{\partial \theta_x}{\partial t} \right)^2 + z_c \frac{\partial v}{\partial t} \frac{\partial \theta_x}{\partial t} - y_c \frac{\partial w}{\partial t} \frac{\partial \theta_x}{\partial t} \right) dx, \tag{13}$$

where  $I_0$  is the polar moment of inertia. The variation of the kinetic energy is then formulated and ordered with respect to the virtual displacement components  $\delta u$ ,  $\delta v$ ,  $\delta w$  and  $\delta \theta_x$ :

$$\begin{aligned} \delta T &= \int_L m \left( \frac{\partial u}{\partial t} \frac{\partial}{\partial t} \delta u + \left( \frac{\partial v}{\partial t} + z_c \frac{\partial \theta_x}{\partial t} \right) \frac{\partial}{\partial t} \delta v \right. \\ &\quad \left. + \left( \frac{\partial w}{\partial t} - y_c \frac{\partial \theta_x}{\partial t} \right) \frac{\partial}{\partial t} \delta w + \left( I_0 \frac{\partial \theta_x}{\partial t} + z_c \frac{\partial v}{\partial t} - y_c \frac{\partial w}{\partial t} \right) \frac{\partial}{\partial t} \delta \theta_x \right) dx. \end{aligned} \tag{14}$$

In order to derive the dynamic motion equations, Hamilton’s principle is used:

$$\delta \int_{t_1}^{t_2} (U - T - W) dt = 0. \tag{15}$$

After some time integrations by parts in the resulting equation and straightforward necessary calculations, the following equations of motion are obtained in elastic domain when the non-linear terms are considered until order 3:

$$-\frac{\partial N}{\partial x} = q_x, \tag{16a}$$

$$m\left(\frac{d^2v}{dt^2} + z_c \frac{d^2\theta_x}{dt^2}\right) + EI_z\left(v^{(4)} + 3v'v''v''' + v''^3 + \frac{v^{(4)}v'^2}{2}\right) - N(v'' + z_c\theta_x'' + y_c(\theta_x\theta_x'' + \theta_x'^2)) + (EI_z - EI_y)(w^{(4)}\theta_x + 2w''' \theta_x' + w''\theta_x'' - v^{(4)}\theta_x^2 - 4v''' \theta_x\theta_x' - 2v''\theta_x\theta_x'' - 2v'\theta_x'^2) = q_y, \tag{16b}$$

$$m\left(\frac{d^2w}{dt^2} - y_c \frac{d^2\theta_x}{dt^2}\right) + EI_y\left(w^{(4)} + 3w'w''w''' + w''^3 + \frac{w^{(4)}w'^2}{2}\right) - N(w'' - y_c\theta_x'' + z_c(\theta_x\theta_x'' + \theta_x'^2)) + (EI_z - EI_y)(v^{(4)}\theta_x + 2v''' \theta_x' + v''\theta_x'' + w^{(4)}\theta_x^2 + 4w''' \theta_x\theta_x' + 2w''\theta_x\theta_x'' + 2w'\theta_x'^2) = q_z, \tag{16c}$$

$$m\left(I_0 \frac{d^2\theta_x}{dt^2} + z_c \frac{d^2v}{dt^2} - y_c \frac{d^2w}{dt^2}\right) + EI_\omega\theta_x^{(4)} - GJ\theta_x'' - \frac{3}{2}EI_t\theta_x'^2\theta_x'' - N(I_0\theta_x'' - y_c(w'' - v''\theta_x) + z_c(v'' + w''\theta_x)) + (EI_z - EI_y)(v''w'' - v''^2\theta_x + w''^2\theta_x) = q_z(e_y - e_z\theta_x), \tag{16d}$$

where  $E$  and  $G$  are the elastic constants.  $I_y$  and  $I_z$  are the inertial moments of the section. In Eq. (16d)  $J$ ,  $I_\omega$  and  $I_t$  denote, respectively, the St Venant, the warping and the higher order shortening constants. The resulting equations of motion (16) have been established by approximating the circular functions ( $\cos \theta_x = 1 - \frac{1}{2}\theta_x^2$ ;  $\sin \theta_x = \theta_x - \frac{1}{6}\theta_x^3$ ). Non-linear relationships between bending moments and curvatures are considered. Assuming static displacements, these equations are reduced to the ones developed for the post-buckling analysis of thin walled elements under axial and lateral loads. In dynamic analysis, these equations permit one to study on the one hand, the linear vibration of beams when the non-linear terms and loads are disregarded. On the other hand, they allow the investigation of small vibration analyses around pre- and post-buckled states which is the aim of this paper non-linear free vibrations as well as forced vibration of thin-walled beams can also be studied.

### 2.3. Reduced differential system for simply supported beams

For simplicity, consider simple boundary conditions. For simply supported beams with free warping, the first overall displacements modes in bending and torsion are assumed as

$$v(x, t) = v_0(t)\sin\left(\pi \frac{x}{L}\right); \quad w(x, t) = w_0(t)\sin\left(\pi \frac{x}{L}\right); \quad \theta(x, t) = \theta_0(t)\sin\left(\pi \frac{x}{L}\right), \tag{17a-c}$$

where  $v_0(t)$ ,  $w_0(t)$  and  $\theta_0(t)$  are the associated displacement amplitudes which are time dependent. Relationships (17) are commonly adopted as approximation for modes of simply supported beams in both static and dynamic analysis [5]. More recently, Di Egidio et al. [6] use modes (17) in non-linear and chaos dynamics. Based on Galerkin’s approach, the partial differential equations derived in Eqs. (16a)–(16d) can be reduced to a non-linear coupled differential system in time domain. After integrations and some reductions, the resulting bending and torsion equations of

motion are obtained in compact form as

$$\begin{aligned} & \frac{mL^2}{\pi^2} \left( \frac{d^2}{dt^2} v_0 + z_c \frac{d^2}{dt^2} \theta_0 \right) + P_z \left( v_0 + \frac{\pi^2}{8L^2} v_0^3 \right) - P(v_0 + z_c \theta_0) + (P_z - P_y) \left( \frac{8}{3\pi} w_0 \theta_0 - \frac{3}{4} v_0 \theta_0^2 \right) = 0, \\ & \frac{mL^2}{\pi^2} \left( \frac{d^2}{dt^2} w_0 - y_c \frac{d^2}{dt^2} \theta_0 \right) + P_y \left( w_0 + \frac{\pi^2}{8L^2} w_0^3 \right) - P(w_0 - y_c \theta_0) \\ & \quad + (P_z - P_y) \left( \frac{8}{3\pi} v_0 \theta_0 + \frac{3}{4} w_0 \theta_0^2 \right) = \frac{32}{\pi^3} M_0, \\ & \frac{mL^2}{\pi^2} \left( I_0 \frac{d^2}{dt^2} \theta_0 + z_c \frac{d^2}{dt^2} v_0 - y_c \frac{d^2}{dt^2} w_0 \right) + I_0 P_\theta \theta_0 + \frac{3\pi^2 EI_t}{8 L^2} \theta_0^3, \\ & - P(I_0 \theta_0 - y_c w_0 + z_c v_0) + (P_z - P_y) \left( \frac{8}{3\pi} v_0 w_0 - \frac{3}{4} \theta_0 v_0^2 + \frac{3}{4} \theta_0 w_0^2 \right) = M_0 \left( \frac{32}{\pi^3} e_y - \frac{8}{\pi^2} e_z \theta_0 \right). \end{aligned} \tag{18a-c}$$

In this differential system,  $P$  is the compressive axial load which is assumed to be constant.  $M_0$  is the maximal bending moment resulting from the lateral load  $q_z$ .  $P_y$ ,  $P_z$ , and  $P_\theta$  are the buckling loads of a simply supported element, bending and pure torsion. They are given by the following relationships:

$$P_y = \frac{\pi^2 EI_y}{L^2}; \quad P_z = \frac{\pi^2 EI_z}{L^2}, \tag{19a, b}$$

$$P_\theta = \frac{1}{I_0} \left( \frac{\pi^2 EI_\omega}{L^2} + GJ \right); \quad M_0 = q_z \frac{L^2}{8}. \tag{19c, d}$$

Now recall that by neglecting the inertia terms in Eq. (18), the static post-buckling behaviour under axial compressive load  $P$  can be derived, by putting ( $M_0 = 0$ ). Similarly, the lateral post-buckling behaviour under bending loads or equivalent bending moment  $M_0$  can easily be derived by setting ( $P = 0$ ). System (18) can be expressed in a more compact form by using matrix notations as

$$[\mathbf{M}]\{\ddot{\mathbf{U}}\} + [\mathbf{K}_e]\{\mathbf{U}\} + \{\mathbf{N}(\mathbf{U}, P, M_0)\} = \{\mathbf{F}\}, \tag{20}$$

where  $\{\mathbf{U}\}^t = \{v_0(t); w_0(t); \theta_0(t)\}^t$

$$[\mathbf{M}] = \frac{mL^2}{\pi^2} \begin{bmatrix} 1 & 0 & z_c \\ 0 & 1 & -y_c \\ z_c & -y_c & 1 \end{bmatrix} \quad [\mathbf{K}_e] = \begin{bmatrix} P_z & 0 & 0 \\ 0 & P_y & 0 \\ 0 & 0 & I_0 P_\theta \end{bmatrix}, \tag{21a, b}$$

$$\{\mathbf{N}(\mathbf{U}, P, M_0)\} = \left\{ \begin{array}{l} -P(v_0 + z_c\theta_0) + P_z\left(\frac{\pi^2}{8L^2}v_0^3\right) + (P_z - P_y)\left(\frac{8}{3\pi}w_0\theta_0 - \frac{3}{4}v_0\theta_0^2\right) \\ -P(w_0 - y_c\theta_0) + P_y\left(\frac{\pi^2}{8L^2}w_0^3\right) + (P_z - P_y)\left(\frac{8}{3\pi}v_0\theta_0 + \frac{3}{4}w_0\theta_0^2\right) \\ -P(I_0\theta_0 - y_cw_0 + z_cv_0) + \frac{3\pi^2}{8}\frac{EI_t}{L^2}\theta_0^3 + (P_z - P_y)\left(\frac{8}{3\pi}v_0w_0 \right. \\ \left. - \frac{3}{4}\theta_0v_0^2 + \frac{3}{4}\theta_0w_0^2\right) + \frac{8M_0}{\pi^2}e_z\theta_0 \end{array} \right\} \quad (21c)$$

$$\{\mathbf{F}\}^t = \left\{ 0; \frac{32M_0}{\pi^3}; \frac{32M_0}{\pi^3}e_y \right\}, \quad (21d)$$

where  $[\mathbf{M}]$  denotes the mass matrix and  $[\mathbf{K}_e]$  is the elastic stiffness matrix. The vector  $\{\mathbf{N}(\mathbf{U}, P, M_0)\}$  includes the non-linear terms. It depends non-linearly on displacements and linearly on the axial force  $P$  and on bending moment  $M_0$ . The vector  $\{\mathbf{F}\}$  is the external load vector. The non-linear static and dynamic analyses of simply supported beams can be investigated by the system (20). The linear vibration of thin-walled elements can be easily deduced and lead to the well-known eigenfrequencies of thin-walled beams with open section derived in Vlasov’s model. For this reason, they are not discussed here.

#### 2.4. Static equilibrium and small vibration formulations

Based on static equilibrium equations derived from system (18), the post-buckling behaviours of thin-walled elements under both axial and lateral loads have been investigated. To analyze the small vibrations close to static equilibrium position, the displacements are assumed to be the sum of a time-dependent and time independent solutions such as

$$\begin{Bmatrix} v_0 \\ w_0 \\ \theta_0 \end{Bmatrix} = \begin{Bmatrix} v_s \\ w_s \\ \theta_s \end{Bmatrix} + \begin{Bmatrix} v_d(t) \\ w_d(t) \\ \theta_d(t) \end{Bmatrix} = \{\mathbf{U}_s\} + \{\mathbf{U}_d\}. \quad (22)$$

In the present study, the dynamic vector components  $\{\mathbf{U}_d\}$  are assumed to be small, but the static solution vector  $\{\mathbf{U}_s\}$ , corresponding to the post-buckled state, are derived for moderate magnitude. The dynamic solution represents a small vibration about a mean static equilibrium configuration. The equations for static pre- and post-buckling equilibrium states are first obtained by disregarding the inertia terms in Eq. (20) in which case the solution to the resulting equation is  $\{\mathbf{U}_s\}$ . The governing equations for small vibrations around a static equilibrium state are derived by substituting (22) into (20) and neglecting the resulting non-linear terms in  $\{\mathbf{U}_d\}$ . The solution procedure adopted to investigate the static solutions and the eigenfrequencies around a known static solution are then ordered in the following system:

$$\begin{cases} [\mathbf{K}_e]\{\mathbf{U}_s\} + \{\mathbf{N}(\mathbf{U}_s, P, M_0)\} = \{\mathbf{F}\}, \\ [\mathbf{M}]\{\ddot{\mathbf{U}}_d\} + [\mathbf{K}_t(\mathbf{U}_s)]\{\mathbf{U}_d\} = \{\mathbf{0}\}, \end{cases} \quad (23a, b)$$

where  $[\mathbf{K}_t(\mathbf{U}_s)]$  denotes the tangent stiffness matrix which includes the elastic stiffness matrix  $[\mathbf{K}_e]$  and the gradient of the vector  $\{\mathbf{N}\}$  in the vicinity of  $\{\mathbf{U}_s\}$ . Now recall that  $\{\mathbf{U}_s\}$  is obtained by solving numerically system (23a) and depends on the applied loads. The Newton–Raphson iteration method is used for this purpose. The matrix  $[\mathbf{K}_t(\mathbf{U}_s)]$  is built using the static solution  $\{\mathbf{U}_s\}$ . System (23b) governs the small vibrations around a given static equilibrium state. Assuming a harmonic motion with the frequency  $\Omega$ , this equation is reduced to the eigenvalue problem:

$$(-\Omega^2[\mathbf{M}] + [\mathbf{K}_t(\mathbf{U}_s)])\{\mathbf{U}_d\} = \{\mathbf{0}\}. \tag{24}$$

Then, the numerical solution of Eqs. (23a) and (24) permits one to study the small vibration of pre- and post-buckled thin-walled elements under axial and lateral loads.

### 2.5. Load–frequency interaction in the case of bisymmetric sections

The approach developed in the previous section can be easily applied for bisymmetric I sections. Analytical closed form solutions can then be derived for the load–frequency interaction in the pre- and post-buckling ranges. Consider a bisymmetric I section under a compressive load  $P$ . According to relationships (18), with  $y_c = z_c = 0$ , the resulting non-linear vibration equations are given by

$$\begin{aligned} \frac{mL^2}{\pi^2} \frac{d^2}{dt^2} v_0 + (P_z - P)v_0 + P_z \left( \frac{\pi^2}{8L^2} v_0^3 \right) + (P_z - P_y) \left( \frac{8}{3\pi} w_0 \theta_0 - \frac{3}{4} v_0 \theta_0^2 \right) &= 0, \\ \frac{mL^2}{\pi^2} \frac{d^2}{dt^2} w_0 + (P_y - P)w_0 + P_y \left( \frac{\pi^2}{8L^2} w_0^3 \right) + (P_z - P_y) \left( \frac{8}{3\pi} v_0 \theta_0 + \frac{3}{4} w_0 \theta_0^2 \right) &= 0, \\ \frac{mL^2}{\pi^2} I_0 \frac{d^2}{dt^2} \theta_0 + I_0 P_\theta \theta_0 + \frac{3\pi^2 EI_t}{8L^2} \theta_0^3 - P I_0 \theta_0 + (P_z - P_y) \left( \frac{8}{3\pi} v_0 w_0 - \frac{3}{4} \theta_0 v_0^2 + \frac{3}{4} \theta_0 w_0^2 \right) &= 0. \end{aligned} \tag{25a-c}$$

Assuming a linear approximation and a harmonic motion with frequency  $\Omega$ , the load–frequency relationships can be carried out in the pre- and post-buckling regions. In the pre-buckling zone, they are formulated with respect to the linear equations, that are uncoupled and lead to

$$\Omega_1^2 = \Omega_z^2 \left( 1 - \frac{P}{P_z} \right); \quad \Omega_2^2 = \Omega_y^2 \left( 1 - \frac{P}{P_y} \right); \quad \Omega_3^2 = \Omega_\theta^2 \left( 1 - \frac{P}{P_\theta} \right), \tag{26a-c}$$

where  $\Omega_y$ ,  $\Omega_z$  and  $\Omega_\theta$  are the eigenvalues of the beam in bending and pure torsion:

$$\Omega_y^2 = \frac{\pi^4 EI_y}{mL^4}; \quad \Omega_z^2 = \frac{\pi^4 EI_z}{mL^4}; \quad \Omega_\theta^2 = \frac{\pi^2}{mL^2 I_0} \left( \frac{\pi^2 EI_\omega}{L^2} + GJ \right). \tag{27a-c}$$

In the post-buckling state, the load–frequency interactions are formulated around static uncoupled solutions  $\{v_s; 0; 0\}^t$ ,  $\{0; w_s; 0\}^t$ ,  $\{0; 0; \theta_s\}^t$ . Consider the first Eq. (25a), the equation for a small vibration around  $v_s$  is

$$\left( -\Omega^2 \frac{mL^2}{\pi^2} + (P_z - P) + 3 \frac{\pi^2}{8L^2} P_z v_s^2 \right) v_d = 0. \tag{28}$$



The non-trivial static solution  $\{v_s; 0; 0\}^t$  is obtained by omitting the inertia term in Eq. (25a) and leads to:

$$v_s^2 = \frac{8L^2}{\pi^2} \frac{(P - P_z)}{P_z} = \frac{8L^2}{\pi^2} \left( \frac{P}{P_z} - 1 \right). \quad (29)$$

The insertion of  $v_s$  in Eq. (28) gives to the load–frequency relationship in the post-buckling range:

$$\Omega_1^2 = 2\Omega_z^2 \left( \frac{P}{P_z} - 1 \right). \quad (30a)$$

Similar analytical calculations are done on Eqs. (25b) and (25c) and yield to:

$$\Omega_2^2 = 2\Omega_y^2 \left( \frac{P}{P_y} - 1 \right), \quad \Omega_3^2 = 2\Omega_\theta^2 \left( \frac{P}{P_\theta} - 1 \right). \quad (30b, c)$$

The  $(\Omega^2/P)$  relationships (26a)–(26c) and (30a)–(30c) are then linear and this is in agreement with the famous Southwell plot [7], that remains valid again in post-buckling range.

### 3. Numerical results

The numerical results presented here concern the free vibrations of pre-buckled and post-buckled elements under compressive or lateral bending loads. Bisymmetric and mono-symmetric steel sections are considered with Young's modulus ( $E = 210$  GPa), shear modulus ( $G = 80.77$  GPa) and a density ( $\rho = 7800$ ). For the sake of clarity, static equilibrium paths are first presented and the eigenvalue variations of the element following the equilibrium curves are discussed. More details on the post-buckling equilibrium paths can be found in Refs. [3,4].

#### 3.1. Vibration of bisymmetric I section under compression

The vibration of bi-symmetric I section have been studied in both the pre- and post-buckling states. All the studied cases have demonstrated that the variation of eigenfrequencies in bending and torsion agree well with relationships (26a), (26c) and (30a), (30c). For this reason they are not presented here. Nevertheless, the analytical load–frequency relationships are derived without any imperfections and are then related to the perfect structure, consider the imperfection effects on post-buckling and eigenvalue variation. The torsion equilibrium curve is selected for this analysis. Equilibrium curves are presented in Fig. 2a, for some initial torsion imperfections (denoted  $\theta_i$ ). In the presence of initial torsion imperfections, the beam behaviour becomes highly non-linear but remains stable. The variation of the pure torsion eigenvalue  $\Omega$  along the equilibrium curves for different imperfections follow in Fig. 2b. In the perfect case, the eigenvalue decreases from the pure torsion eigenvalue  $\Omega_\theta = 163$  to zero when the buckling load  $P_\theta = 1768$  is reached. This eigenvalue increase in the post-buckling state and remains positive. In the presence of imperfections, all the pure torsion eigenvalues decrease in the pre-buckling state from  $\Omega_\theta$  to a minimum non-vanishing value, which is a function of the imperfection amplitude, and then increases in the post-buckled state.

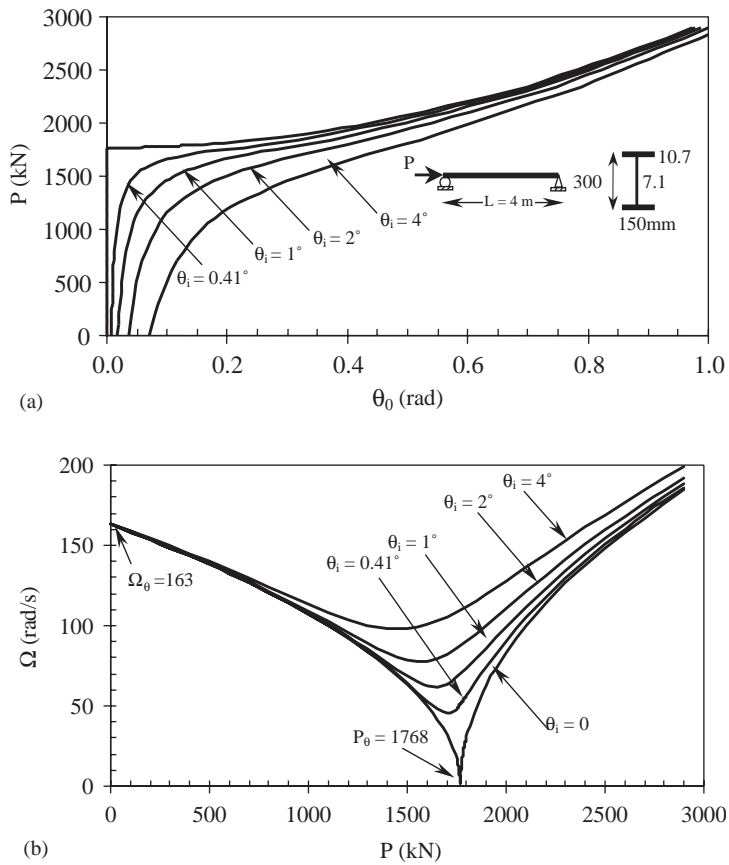


Fig. 2. (a) Torsion imperfection effects on the torsion post-buckling behaviour of a compressed I beam. (b) Torsion imperfection effects on load–frequency variation of a compressed I beam.

### 3.2. Vibration of T section beams under compression

The second example concerns a T beam under compressive load. The buckling behaviour of this section has been investigated and shows that the first buckling mode is always flexural–torsional. The post-buckling equilibrium curve ( $P, \theta_0$ ) is presented in Fig. 3a for a beam of length  $L = 2$  m. One can remark that the torsion angle is present only in the post-buckling state and the equilibrium path is symmetric. The flexural–torsional buckling load value is 222 kN. A limit point is present in the post-buckling state for a load  $P = 290$  kN. For the vibration analysis, the eigenvalues of the beam have been computed following the equilibrium path from  $P = 0$  until the buckling load  $P = 222$  kN. In the post-buckling region, only the positive part of the curve ( $\theta_0 > 0$ ) is considered.

The variation of the lower eigenvalue with respect to the load  $P$  is shown in Fig. 3b in both pre- and post-buckling states. In the pre-buckling zone, this eigenvalue decreases linearly from the fundamental frequency  $(191.49)^2$  to zero when the buckling load  $P = 222$  kN is reached. In the post-buckling region, this value increases non-linearly in the stable part of the curve until the limit

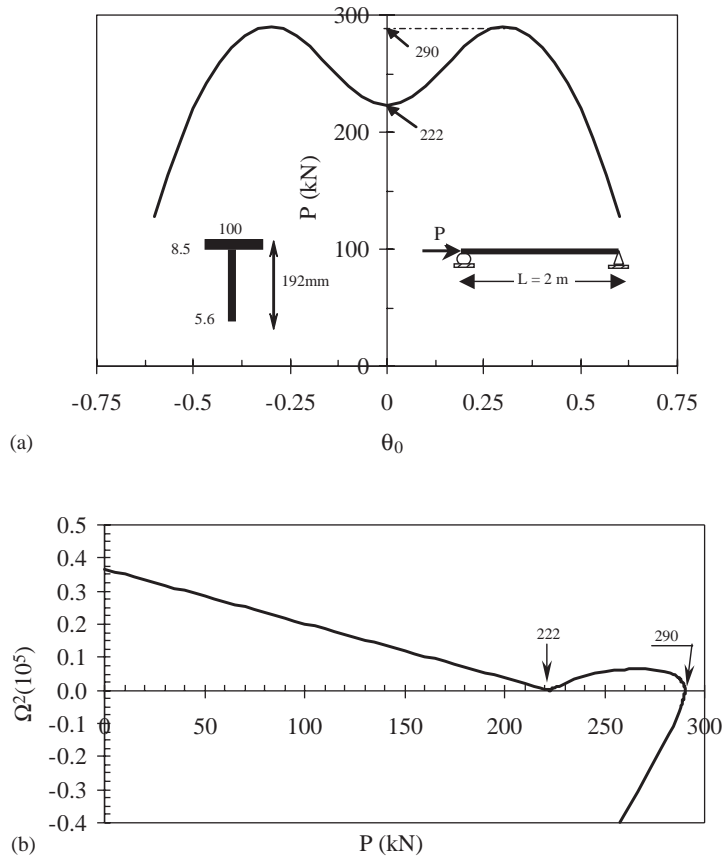


Fig. 3. (a) Post-buckling behaviour of Te beam under axial load  $P$ . (b) Lower eigenvalue variation of a Te section beam under compressive load  $P$ .

point in which  $(\Omega)^2$  vanishes again and then becomes negative in the unstable part of the curve. In fact, in the unstable zone, the eigenvalue is a pure complex number. In the pre-buckling region, the variation is linear and is in good agreement with the analytical solutions (26). In the post-buckling region all the equation of motions are non-linear and highly coupled. The analytical solutions (30) are no longer valid. This test shows that at a bifurcation or a limit point, the lower eigenvalue vanishes. In the post-buckling region, the lower eigenvalue is real in presence of stable equilibrium path and becomes pure complex imaginary in the unstable region. This is in accordance with the well-known Liapunov stability criteria.

### 3.3. Vibration of beams in lateral buckling behaviour

The last example is devoted to the vibration of bisymmetric I beams in lateral buckling. Consider a beam under uniformly distributed lateral load. The load is applied with initial eccentricity  $e_z$  from the shear centre (Fig. 4a). The non-linear behaviour of such beams has been investigated and it has been established that the lateral buckling load depends on the load

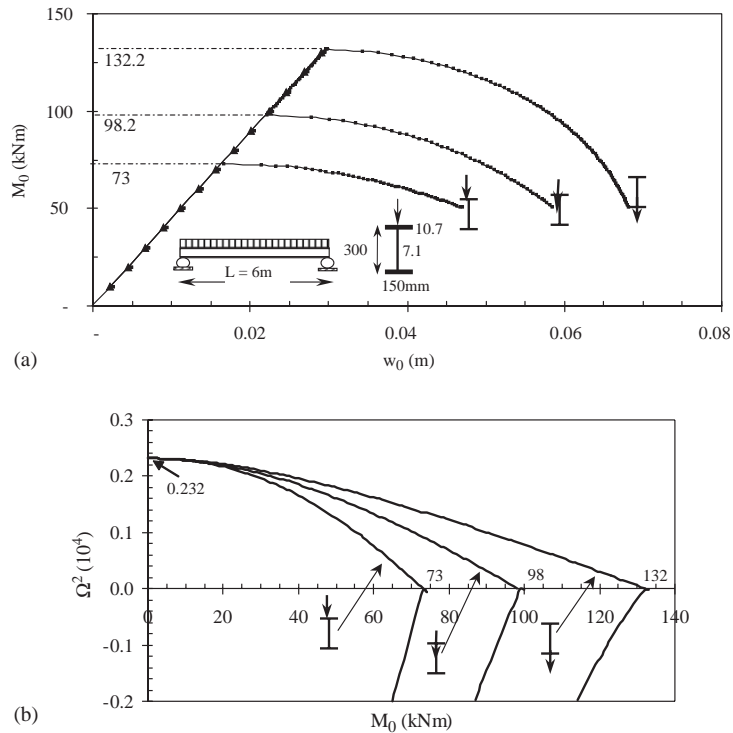


Fig. 4. (a) Equilibrium paths ( $M_0, w_0$ ) in the fundamental and post-buckling state, for some load heights. (b) Variation of the first eigenvalue as function of load and some load heights.

eccentricity  $e_z$ . The effect of this term on lateral buckling resistance of beams has been extensively studied in literature and was called the load height parameter. For the present study, the bisymmetric I section previously studied in Section 3.1 is considered with slenderness length  $L = 6$  m. According to the analytical solutions as formulated in Ref. [4], the lateral buckling moments of this section beam are, respectively, 132 kNm when the load is applied on the bottom flange, 98 kNm for a load on the shear centre, and 73 kNm for a load on the top flange.

In linear vibration, the fundamental eigenfrequencies are computed according to relationships (36a)–(36c), are, respectively,  $\Omega_z = 48.13$ ,  $\Omega_\theta = 90.02$  and  $\Omega_y = 175.35$  rad/s. The moment–deflection curves ( $M_0, w_0$ ) in the pre- and post-buckling regions are presented in Fig. 4a for the three load heights. In the pre-buckling state, this curve is linear and independent of the load height parameter. In the post-buckling region, the load height parameter affects highly the beam response. The variations of the lower eigenvalue as a function of the bending moment  $M_0$  are presented in Fig. 4b in the pre- and post-buckling zones, for the three load heights. In the pre-buckling region, these curves decrease from the lower fundamental eigenvalue  $\Omega_z^2 = 48.13^2$  to zero, when the buckling moment is reached, depending on the position of the load height. The buckling moments associated to the static behaviour are well reproduced in the load–frequency interaction. Due to the unstable nature of the post-buckling state, the square of the eigenvalues becomes negative in the post-buckling region. The relating frequencies are then pure complex imaginary. The load–frequency curves are not linear and depend on the load height parameter in

both pre- and post-buckling regions. Relationships (42) and (45) are no longer valid in the case of beams in lateral buckling. Attard et al. [2] investigated the load frequency interaction of cantilevers as a function of the load height parameter in the pre-buckling state and observed the same phenomenon. Their study is restricted to the pre-buckling state.

#### 4. Conclusions

The vibration behaviour of pre-buckled and post-buckled thin-walled beams with open sections has been investigated. Based on a non-linear model which accounts for non-linear warping, bending–bending and torsion–bending couplings, the non-linear dynamic equations have been formulated. The model has been applied to the investigation of load–frequency interaction of struts under compression or beams under lateral bending loads, in pre- and post-buckling ranges.

In the case of a strut under compressive load  $P$ , closed-form linear eigenvalue curves ( $\Omega^2/P$ ) have been obtained, in the pre- and post-buckling regions, especially for bi-symmetric sections. This linearity also holds good in the case of mono-symmetric sections, but only in the pre-buckling region. In the post-buckling zone, the governing equilibrium equations of mono-symmetric sections are non-linear and highly coupled, so the derivation of the analytical solutions can be cumbersome. For this reason, only numerical solutions are discussed. The load–frequency interaction has to be analyzed carefully, according to section shape and beam length. As expected, the lowest eigenvalue  $\Omega^2$  decreases linearly in the pre-buckling region and vanishes at buckling or limit load. Clearly, in the post-buckling range, the load–frequency curve depends on the nature of the equilibrium path. The eigenvalue  $\Omega^2$  is positive when the solution is stable and negative when it is unstable. Beams with bisymmetric I sections and preloaded in lateral buckling have also been investigated. In this case, the eigenfrequencies are load-height dependent and the load–frequency curves are non-linear even in the pre-buckling range. Moreover, the first eigenvalue is negative in the post-buckling range, which means that the equilibrium is unstable. It is then proved that the load–frequency interaction is more significant for the lower eigenvalue of the beam.

#### References

- [1] R.S. Barsoum, Finite element method applied to the problem of stability of a non-conservative system, *International Journal for Numerical Method in Engineering* 3 (1971) 63–87.
- [2] M.M. Attard, I.J. Somerville, Stability of thin-walled open beams under nonconservative loads, *Mechanics of Structures and Machines* 15 (1987) 395–412.
- [3] F. Mohri, L. Azrar, M. Potier-Ferry, Flexural–torsional post-buckling analysis of thin-walled elements with open sections, *Thin-Walled Structures* 39 (2001) 907–938.
- [4] F. Mohri, L. Azrar, M. Potier-Ferry, Lateral post-buckling analysis of thin-walled open section beams, *Thin-Walled Structures* 40 (2002) 1013–1036.
- [5] J.J. Thomsen, *Vibrations and Stability: Order and Chaos*, McGraw-Hill, London, 1997.
- [6] A. Di Egidio, A. Luongo, F. Vestroni, A non-linear model for the dynamics of open cross-section thin-walled beams. Part I: formulation, *International Journal of Non-Linear Mechanics* 38 (2002) 1067–1082.
- [7] R.V. Southwell, On the analysis of experimental observations in problems of elastic stability, *Proceedings of the Royal Society of London* 135 (1932) 601–616.